J Mater Sci (2008) 43:3531–3538
DOI 10.1007/s10853-008-2541-1

Glasses and glass-ceramics in the $SrO–TiO_2–Al_2O_3–SiO_2–B_2O_3$ system and the effect of P_2O_5 additions

Murat Bengisu · Richard K. Brow · Andrew Wittenauer

Received: 14 September 2007 / Accepted: 7 February 2008 / Published online: 22 March 2008

Abstract The glass formation abilities of various compositions in $SrO–TiO_2–Al_2O_3–SiO_2$, $SrO–TiO_2–B_2O_3–SiO_2$, $SrO–TiO_2–Al_2O_3–B_2O_3$, and $SrO–TiO_2–Al_2O_3–SiO_2–B_2O_3$ systems were studied. Many new compositions were found to be suitable for the casting of crack-free, optically clear glasses of different color and with glass transition temperatures ranging from 595 to 775 °C. The crystallization behavior, structure, and thermal expansion behavior of selected glasses were analyzed by DTA, XRD, dilatometry, and heat treatment. The effect of P_2O_5 on the glass structure and crystallization behavior was also studied. P_2O_5 played a dual role depending on composition. In some glasses it acted as a nucleating agent while in others it suppressed crystallization. Heat treatment of borate and borosilicate glasses transformed them into glass-ceramics while comparable $SrO–TiO_2–Al_2O_3–SiO_2$ glasses showed a lower tendency to crystallize and form glass-ceramics under the same conditions.

Introduction

Borate-based glasses have various current and potential engineering applications. Some of the more significant ones are low-temperature, specialty sealing [1–3], fast ionic conductors for use in solid-state lithium batteries [4, 5], and radiation and thermoluminescence dosimetry devices [5]. Interest in $SrTiO_3$ glasses and glass-ceramics stems from the ferroelectric properties of $SrTiO_3$ with perovskite structure. $SrTiO_3$ is thought to be a promising candidate for future microelectronic devices [6]. Glass-ceramics based on $SrTiO_3$ were used as cryogenic capacitive temperature sensors and they offer the possibility to be used in several other applications requiring temperature compensation of the dielectric constant [7, 8]. Glass-ceramics in the strontium titanate aluminosilicate and strontium titanate borosilicate systems exhibit interesting dielectric properties [9–11]. SrO containing aluminoborate glasses were recently studied for sealing applications in solid oxide fuel cells [12]. Some of the present authors' preliminary results also indicated that these glasses may be used to seal $SrTiO_3$—based ceramics to themselves or other materials with similar thermal expansion properties. While independent research groups have studied some glasses containing $SrTiO_3$, this study aims to look into these glasses from a more comprehensive and systematic perspective. In addition to some of the previously studied compositions in the $SrO–TiO_2–Al_2O_3–SiO_2$ [8, 13, 14], $SrO–TiO_2–B_2O_3–SiO_2$ [9, 15], and $SrO–TiO_2–Al_2O_3–B_2O_3$ systems [11, 16], new glasses were formed in those three systems. The $SrO–TiO_2–Al_2O_3–SiO_2–B_2O_3$ system was also studied. The glass and glass-ceramic formation capabilities of 13 compositions in these systems have been investigated. In selected systems, some physical, crystallographic, and microstructural information has been derived. The effect of P_2O_5 addition on glass structure and properties in selected glasses was also analyzed. An important effect of P_2O_5 is to significantly improve the chemical durability of some of the glasses studied in this

M. Bengisu
Department of Industrial Engineering, Eastern Mediterranean University, Famagusta, Northern Cyprus

Present Address:
M. Bengisu (✉)
Department of Industrial Engineering, Yasar University, Kazim Dirik Mah. 364 Sok., No:5 Bornova, Izmir 35500, Turkey
e-mail: murat.bengisu@gmail.com

R. K. Brow · A. Wittenauer
Department of Materials Science & Engineering, University of Missouri-Rolla, 223 McNutt Hall, Rolla, MO 65409, USA

article. This effect was discussed in detail in a separate paper [17]. The corrosion rate of $SrTiO_3$–aluminoborate glasses decreased by over two orders of magnitude with the addition of up to 9 mol% P_2O_5. Here, the effect of P_2O_5 on glass transition and crystallization will be discussed.

Experimental procedure

Preparation of glasses and glass-ceramics

Batches of 20 g were prepared by mixing the necessary amounts (with a weight tolerance of ±1 mg) of powder materials and lightly grinding them to mix and reduce inhomogeneities. Reagent grade $SrCO_3$ (Mallinckrodt), TiO_2 (Fisher), H_3BO_3 (Fisher), Al_2O_3 (Aldrich), fused quartz (Particle Processing & Classifying Corp.), and P_2O_5 (Aldrich) were used to obtain the glass formulations listed in Table 1. P_2O_5 was weighed immediately after removal from sealed containers to reduce the error due to water absorption. Powder mixtures were calcined in Pt crucibles at 1,000 °C for 10 min. This was followed by a fast ramp to the peak temperature and a 2 h soak to allow homogenization of the molten glass. The peak temperatures that allowed a low enough viscosity for casting of glasses under investigation are shown in Table 1. Molten glass was poured into preheated graphite molds at ~500 °C, annealed at 550 °C for 1 h, and furnace-cooled to ambient temperature. Stress analysis with polarized light indicated that the glass bars were practically free of residual stress after the heat treatment.

Glass pieces were placed on alumina substrates for heat treatment in order to study glass-ceramic formation. Compositions from the G2, G8, and G12 categories were heat treated in a box furnace in air for 1 h. Heat treatment was applied at approximately 100, 200, and 300 °C above the glass transition temperature of each composition in triplicate. Each heat treatment lasted for an hour at the peak temperature.

Table 1 Nominal and final compositions, process temperatures, and colors of $SrTiO_3$-aluminoborate, $SrTiO_3$-aluminosilicate, and $SrTiO_3$-aluminoborosilicate glasses with P_2O_5 additions

Sample	Composition (mol%)						Other	Process temp. (°C)	Glass formation	Color
	SrO	TiO_2	B_2O_3	SiO_2	Al_2O_3	P_2O_5				
G1	10	10	53.33	0	26.67	0	0	1450	Yes	Clear
G2	15	15	46.66	0	23.34	0	0	1450	Yes	Gold brown
G2[a]	*15.8*	*17.9*	*31.3*	*0.6*	*33.5*	*0*	*0.9*			
G2P3	15	15	45	0	22	3	0	1450	Yes	Gold brown
G2P3[a]	*12.6*	*16.6*	*34.0*	*1.2*	*30.5*	*3.7*	*1.4*			
G2P6	15	15	43.5	0	20.5	6	0	1450	Yes	Gold brown
G2P9	15	15	42	0	19	9	0	1450	Yes	Gold brown
G3	20	20	40	0	20	0	0	1450	Excessive crystallization	
G4	10	10	26.67	53.33	0	0	0	1650	No melting	
G5	15	15	23.34	46.66	0	0	0	1650	Melts but too viscous	
G6	20	20	20	40	0	0	0	1650	No melting	
G7	10	10	0	53.33	26.67	0	0	1650	No melting	
G8	15	15	0	46.66	23.34	0	0	1650	Yes	Dark brown
G8[a]	*8.2*	*12.4*	*0*	*49.2*	*29.8*	*0*	*0.4*			
G8P3	15	15	0	45	22	3	0	1650	Yes	Dark brown
G8P6	15	15	0	43.5	20.5	6	0	1650	Yes	Dark brown
G9	20	20	0	40	20	0	0	1650	No melting	
G10	10	10	26.67	26.66	26.67	0	0	1600	Yes	Light brown
G10P3	10	10	25.67	25.66	25.67	3	0	1600	Yes	Light brown
G10P3[a]	*6.4*	*9.2*	*23.4*	*27.2*	*30.0*	*3.0*	*0.8*			
G10P6	10	10	24.67	24.66	24.67	6	0	1600	Yes	Light brown
G11	15	15	23.33	23.33	23.34	0	0	1650	Melts but too viscous	
G12	20	20	20	20	20	0	0	1600	Yes	Dark blue
G12[a]	*16.1*	*18.0*	*21.8*	*19.4*	*23.8*	*0.0*	*0.9*			
G12P3	20	20	19	19	19	3	0	1600	Yes	Dark blue

[a] Italicized values indicate resulting composition according to XRF analysis when available

Differential thermal analysis and dilatometry

Differential thermal analysis (DTA) was performed with a Perkin-Elmer DTA-7 instrument using powder samples and a 10 °C/min heating rate. A narrow particle size range (75–88 μm) and equal mass (70 ± 0.1 mg) were used for all samples. DTA measurements were performed using a Pt crucible under flowing nitrogen gas. The glass transition temperature of each composition (T_g) was determined from the points of intersection of extended lines at the glass transition shoulder in the DTA track.

Coefficients of thermal expansion (CTE) were measured using ~25 mm long glass bars with parallel ends obtained by grinding with SiC paper. An Orton Model 1600 dilatometer was used to determine thermal expansion in air at a heating rate of 3 °C/min. The dilatometric softening point (T_d) was determined from the temperature corresponding to the peak point of dilatation. The error in CTE and T_d measurements is estimated as $\pm 3 \times 10^{-7}$/°C and ±3 °C, respectively [18].

X-ray powder diffraction

X-ray diffraction (XRD) was used to check the presence of any crystal phase in the as-cast glass samples. Powder samples were also studied by XRD after DTA runs in order to characterize crystalline phases and for the analysis of phase evolution in glass-ceramics. A Scintag LET 2400 X-ray diffractometer was used. Each sample was scanned at 2 theta angles from 15 to 70°.

X-ray fluorescence

X-ray fluorescence (XRF) was used to verify the compositions of selected glasses. Standardless, semi-quantitative analysis was performed at the Turkish National Research Council facilities using a Philips PW-2404 wavelength dispersive XRF device. Four-centimeter diameter pellets pressed from powdered glass were used for analysis. The error in standardless XRF of glass samples is typically within ±5% [19]. The amount of B_2O_3 was calculated from the difference between 100% and the "sum before normalization" in the case of borate containing compositions.

Microhardness and density

Vickers microhardness values were determined with a Tronic HVS-1000 instrument. Polished samples were subjected to a load of 200 g at an indentation time of 15 s. The average of four microhardness values per sample are reported. The highest experimental variation was ±8%. Density was measured from by the Archimedes principle in water using a digital balance with a precision of 0.01 g. The average density, based on measurements from two different regions, is reported for each type of glass. The experimental variation was in the order of ±3%.

Results

Table 1 shows the nominal compositions investigated in this study, resulting compositions determined by XRF analysis, and the ability to obtain useful glass samples with them. There is reasonable agreement between nominal and measured compositions in the case of glasses prepared at 1,450 °C. Compositional changes occurred at $T > 1{,}600$ °C, probably due to volatilization. The highest amount of impurities in measured compositions was 1.2 mol% SiO_2 (in nominally silica free glass) and 0.6 mol% Fe_2O_3 (Table 1). These impurities may have originated from the furnace environment during melting. As seen in the table, some compositions resulted in a clear glass while others crystallized after casting. Some compositions did not melt at up to 1,650 °C or the high viscosity did not allow casting.

Table 2 summarizes microhardness, density, and CTE data as well as glass-transition and crystal formation temperatures obtained from DTA experiments in these glasses. CTE values at the temperature range 200–500 °C vary between 5.1×10^{-6}/°C and 7.5×10^{-6}/°C. The microhardness increases roughly with the relative SiO_2 content in the glass (see Tables 1 and 2) as expected, since SiO_2 provides a three-dimensional network while the basic building block of B_2O_3 glasses is planar [20]. For example, microhardness values corresponding to G2, G12, G10, and G8 glasses with a SiO_2 content of 0, 20, 27, and 47 mol% are 639, 684, 709, and 728, respectively. Obviously, the relative content of modifier and intermediary oxides in different compositions complicates this analysis. Nevertheless, the microhardness values of non-silica borate glasses are in agreement with comparable data from the literature [21, 22].

$SrO–TiO_2–B_2O_3–Al_2O_3$ compositions (G1–G3)

Among the three $SrO–TiO_2–B_2O_3–Al_2O_3$ compositions, the G2 composition resulted in the best glasses since these had low viscosity at the casting temperature, which facilitated casting, and they exhibited high thermal shock, that is, low tendency to fracture during fast cooling in the mold. G1 glass could not be cast without cracks and G3 glass crystallized rapidly under similar casting conditions. G1 glasses were clear and G2 glasses had a golden brown color. The addition of P_2O_5 to G2 compositions decreased the viscosity at the same process temperature as observed

Table 2 Some physical and mechanical properties of $SrTiO_3$-aluminoborate, $SrTiO_3$-aluminosilicate, and $SrTiO_3$-aluminoborosilicate glasses and the effect of P_2O_5 additions

Sample	H_v^a (kg/mm^2)	ρ^b (g/cm^3)	$T_g^{c,d}$ (°C)	$T_d^{c,e}$ (°C)	$CTE^{f,g}$ x 10^{-6}/°C	1st Peak[h] (°C)	2nd Peak (°C)	3rd Peak (°C)	4th Peak (°C)	1st Peak Height (mW)	$(\delta T)_p^i$ (%)
G1	687	2.61	629	N/A	N/A	745	–	–	–	–	–
G2	639	2.98	625	682	6.82	701	777	–	–	24.42	Reference
G2P3	592	2.80	610	670	6.56	686	810	–	–	17.36	−29%
G2P6	599	2.75	600	660	6.79	666	Suppressed	–	–	26.56	9%
G2P9	–	–	595	648	6.60	668	726	–	–	8.86	−64%
G8	728	2.99	775	–	5.87	847	1042	–	–	6.49	Reference
G8P3	632	2.91	755	–	5.65	834	1080	–	–	1.31	−80%
G8P6	806	3.10	752	–	6.14	830	Suppressed	–	–	4.91	−24%
G10	709	2.75	690	758	5.43	820	–	–	–	143.42	Reference
G10P3	715	2.72	675	741	5.78	845	–	–	–	27.26	−81
G10P6	668	2.67	667	740	5.12	922	–	–	–	4.66	−97
G12	684	3.11	660	699	7.25	719	792	864	1126	17.43	Reference
G12P3	747	3.04	655	694	7.47	715	774	Suppressed	Suppressed	10.87	−38

[a] Vickers microhardness

[b] Density

[c] ±2 °C

[d] Glass transition temperature

[e] Dilatometric softening point

[f] 200–500 °C, no crystal phase

[g] Coefficient of thermal expansion

[h] Crystallization peaks observed in DTA, ±1 °C

[i] Change in the first peak height upon P_2O_5 addition

during casting. No significant color change occurred with P_2O_5 additions to G2 glasses. When G2 and G2P3 glasses were cast into a mold, the free surface not in contact with the mold, that is, the slowest cooled region, crystallized and formed a white layer. One additional composition in this system, namely 42.1 SrO, 20 TiO_2, 30.9 B_2O_3, and 7 Al_2O_3 (in mol%), was identical to one of the 15 compositions reported by Klyuev et al. [16]. This glass, selected for comparative purposes, was a clear glass and it could be cast without cracking or crystallization. The same melting temperature reported by Klyuev et al. (1,450 °C) was used in G1–G3 compositions, which was observed to be a suitable temperature for melting and casting.

SrO–TiO_2–B_2O_3–SiO_2 compositions (G4–G6)

G4–G6 compositions did not melt at 1,227 °C (1,500 K), which is the melting temperature reported for identical (G6) or similar (G4 and G5) compositions [9]. G4 and G6 compositions were heated up to 1,650 °C but no melting occurred. G5 compositions did not melt below ~1,600 °C. Even at this temperature a gray mixture formed with a very high viscosity, preventing casting.

SrO–TiO_2–Al_2O_3–SiO_2 compositions (G7–G9)

No melting occurred up to 1,650 °C in the case of compositions G7 and G9. However, a melt with relatively high viscosity formed at 1,650 °C with the G8 composition, which formed a dark brown glass without cracking or crystallization upon pouring. Addition of 3–6 mol% P_2O_5 to G8 glasses decreased the viscosity during casting.

SrO–TiO_2–Al_2O_3–SiO_2–B_2O_3 compositions (G10–G12)

In this compositional range, G11 melted, but it had a very high viscosity at 1,650 °C, which prevented pouring. On the other hand, compositions G10 and G12 were fluid enough at the same temperature and formed light brown and blue colored glasses, respectively, upon pouring. No significant viscosity change could be observed during casting of P_2O_5 containing G10 and G12 compositions. Addition of up to 6 mol% P_2O_5 to G10 glasses did not visibly change the color. No cracking or crystallization occurred in G10, G10P3, or G10P6 compositions. Some surface crystallization occurred on the slower cooled regions of glasses with G12 and G12P3 compositions.

Discussion

Glass formation and structural properties

SrO–TiO$_2$–B$_2$O$_3$–Al$_2$O$_3$ compositions (G1–G3)

Among the three glasses prepared in this range, G1, which has a higher amount of B_2O_3 and lower amount of SrO as well as TiO_2, exhibited cracking upon cooling, while G2 could be cast with no cracking. This indicates that the thermal shock resistance of G1 glass is lower compared to G2. Thermal shock resistance is a function of tensile strength, Poisson ratio, Young's modulus, and CTE [23]. Since most of these data are not available for both compositions, no further discussion would be suitable regarding thermal shock properties.

The glass transition temperatures, temperatures of crystalline phase formation, and thermal expansion coefficients (CTE's) of SrO–TiO_2–B_2O_3–Al_2O_3 glasses with and without P_2O_5 are given in Table 2. The glass transition temperatures of these glasses are between 595 and 630 °C and the lowest among all glass families analyzed in this study. As seen from Table 2, T_g and T_d values decreased consistently as the P_2O_5 content increased. This indicates a decrease in viscosity (also supported from observations during casting) and a decrease in cross-linking in the glass structure [20]. The decreasing density with increasing P_2O_5 content (Table 2) further supports this viewpoint.

A decrease in T_p (crystallization temperature) also occurred with increasing P_2O_5 content (Table 2 and Fig. 1). Consistently lower T_p values indicate an increased concentration of nuclei in the glass, suggesting that P_2O_5 acts as a nucleating agent [24].

SrO–TiO$_2$–B$_2$O$_3$–SiO$_2$ compositions (G4–G6)

No glass could be obtained in this compositional range as mentioned in the "Results" section.

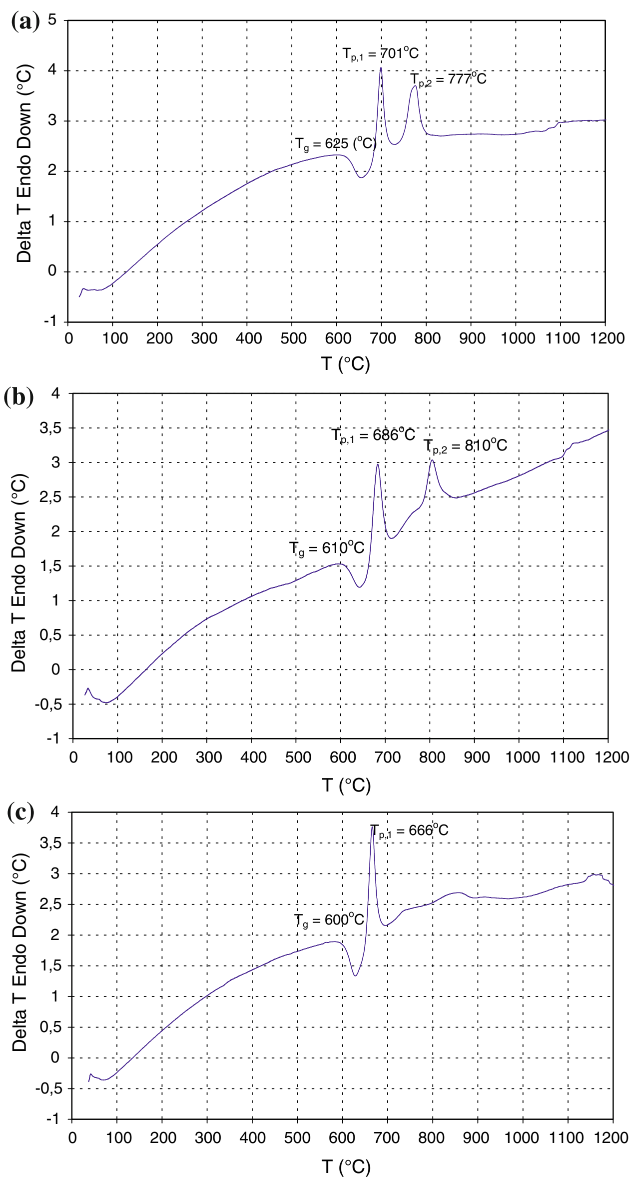

Fig. 1 DTA curves of (**a**) G2, (**b**) G2P3, and (**c**) G2P6 glasses

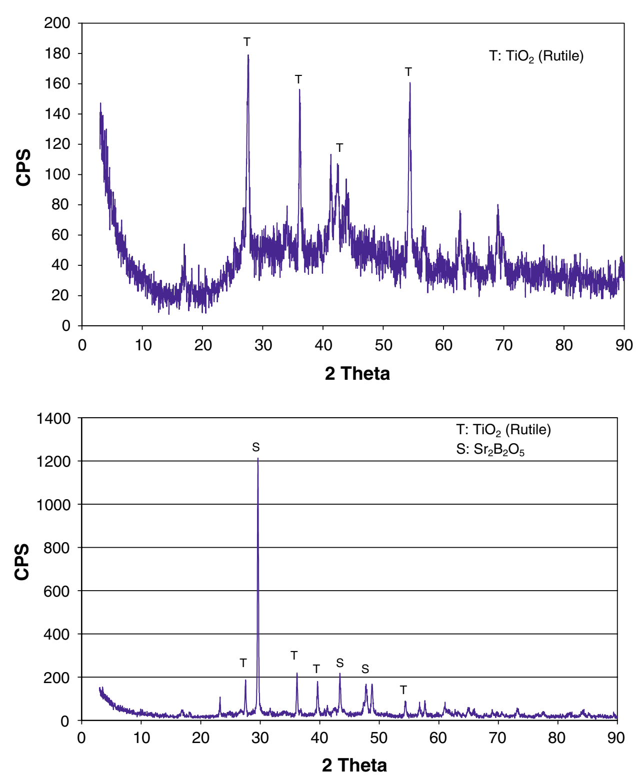

Fig. 2 XRD spectra of (**a**) G2 glass heat treated for 1 h at 750 °C and (**b**) G1 glass heat treated for 1 h at 850 °C

Table 3 Heat treatment temperatures and resulting properties

Sample	Initial color	T1 (°C)	Resulting appearance[a]	Wetting[b]	Crystalline phases	T2 (°C)	Resulting appearance[a]	Wetting[b]	Crystalline phases	T3 (°C)	Resulting appearance[a]	Wetting[b]
G1	Clear	750	Light blue, glossy, shape retained	No	Not analyzed	850	White, glossy, shape retained	No	$Sr_2B_2O_5$, TiO_2 (Rutile)	950	White, matte, shape retained	No
G2	Gold brown	750	Light blue, glossy, shape retained	No	$Sr_2B_2O_5$, TiO_2 (Rutile)	850	White, glossy, shape retained	No	Not analyzed	950	White, matte, shape retained	No
G2P3	Gold brown	750	Light blue-white, glossy	Yes	$Sr_2B_2O_5$, TiO_2 (Rutile)	850	White, glossy	Yes	Not analyzed	950	White, matte, some shape change	No
G2P6	Gold brown	750	Light blue, glossy, some shape change	Yes	TiO_2 (Anatase)	850	White, glossy, total melting	Yes	Not analyzed	950	White, matte, total melting	Wk
G8	Dark brown	870	Dark blue (transparent)	No	Small amount of Rutile	970	Light blue, semi-transparent, shape retained	No	Not analyzed	1050	Light blue, glossy, shape retained	No
G8P3	Dark brown	850	Dark blue (transparent)	No	Not analyzed	950	Light blue, semi-transparent, shape retained	No	Not analyzed	1050	Light blue, glossy, shape retained	No
G8P6	Dark brown	850	Blue (transparent)	No	Not analyzed	950	Light blue, transparent, shape retained	No	Not analyzed	1050	White with some blue tint, glossy, shape retained	No
G10	Light brown	800	Blue, glossy, shape retained	No	$Sr_2B_2O_5$, $Sr_2Ti_2O_7$, TiO_2 (Rutile)	900	Light blue, glossy, shape retained	No	Not analyzed	1000	White, glossy, shape retained	No
G10P3	Light brown	800	White, glossy	No	Not analyzed	900	White, glossy	Wk	Not analyzed	1010	White, glossy	Wk
G10P6	Light brown	800	White, glossy	No	Not analyzed	900	White, glossy	Wk	Not analyzed	1010	White, glossy	Yes
G12	Dark blue	770	Blue, glossy, shape retained	No	$SrAl_2Si_2O_8$ (Hexacelsian), TiO_2 (Anatase, Rutile)	870	White, glossy, shape retained	No	Not analyzed	970	White, glossy, shape retained	No
G12P3	Dark blue	750	Phase separated region light blue, the rest transparent	No	TiO_2 (Anatase, Rutile)	850	White, glossy	Yes	TiO_2 (Anatase, Rutile)	950	White, matte, rough surface	No

[a] Unless otherwise indicated, samples are opaque

[b] Al_2O_3 substrate; No, no wetting; Yes, strongly attached; Wk, weak attachment

$SrO–TiO_2–Al_2O_3–SiO_2$ compositions (G7–G9)

Similar to G2 glasses, P_2O_5 acts as a crystallization enhancer in G8 glasses, demonstrated by a lowering of T_p upon increased P_2O_5 content (Table 2). T_g values decreased also in these glasses consistently as the P_2O_5 content increased.

$SrO–TiO_2–Al_2O_3–SiO_2–B_2O_3$ compositions (G10–G12)

As mentioned in the Results section, G10 glass is light brown, while G12 glass is blue colored. The differences in color in these two glasses may be an indication of different coordination numbers of the transition metal Ti [25].

The trend with T_g and T_d values are similar in G10 and G12 glasses (Table 2) with similar implications discussed for G2 glasses. With increased P_2O_5 additions to G10 glasses, $(\delta T)_p$ decreased while T_p increased (Table 2). Both of these phenomena indicate a decreased concentration of nuclei in the glass suggesting that P_2O_5 enhances the glass forming tendency in G10 glasses (contrary to G2, G8, and G12 glasses) and suppresses the nucleating rate. In fact, the dual role of P_2O_5 as a promoter of crystallization or an enhancer of glass formation is well-known [24].

Crystallization and glass-ceramic formation

According to X-ray data, rutile (TiO_2) and $Sr_2B_2O_5$ crystallize during heating between 700 and 850 °C in G1 and G2 glasses (Fig. 2 and Table 3). DTA analysis of these two glasses indicated that crystallization does not start until 745 °C in G1 and only one phase crystallizes during rapid heating, while two crystallization peaks occur in G2; one of them at 701 °C and the other at 777 °C (Fig. 1).

Comparison of DTA curves of G12 and G12P3 glasses indicated that a third crystal peak that appears in G12 is suppressed in G12P3. XRD analysis showed that G12 contains hexacelsian ($SrAl_2Si_2O_8$), rutile (TiO_2), and anatase (TiO_2), while G12P3 contains only rutile and anatase after heat treatment at 800 °C for 1 h (Table 3). Thus, it seems that P_2O_5 suppresses hexacelsian formation.

Heat treatment of G2, G10, and G12 compositions at all three temperatures mentioned above resulted in glass-ceramics as determined by XRD and by the opaque appearance. On the other hand, although DTA studies showed some crystallization peaks in G8 glasses, the tendency for crystallization, especially for the phase that forms first, is not as strong as in G2, G10, or G12 glasses. This fact is also represented by comparison of DTA results obtained under similar conditions. While DTA scans indicate a sharp peak for G2 glass, the peak is blunt in the case of G8 glass (see 1st peak heights, Table 2), showing lower tendency for crystallization and glass-ceramic formation. It was however possible to obtain opaque glass-ceramics in G8 glasses at higher temperatures.

The addition of P_2O_5 to G2 compositions decreased the softening temperature based on observations summarized in Table 3 as should be expected from T_g values obtained from DTA analysis (Table 2). P_2O_5 containing G2 compositions also exhibited wetting of the alumina substrate, unlike the base G2 glass, as listed in Table 3. On the other hand, addition of 6 mol% P_2O_5 to G8 compositions limited the glass to glass-ceramic transformation under similar conditions. This observation parallels DTA results where the second peak in G8P6 glass is suppressed, compared to the G8 glass.

Summary and conclusions

New glasses and glass-ceramics in $SrO–TiO_2–Al_2O_3–SiO_2$, $SrO–TiO_2–B_2O_3–SiO_2$, $SrO–TiO_2–Al_2O_3–B_2O_3$, and $SrO–TiO_2–Al_2O_3–SiO_2–B_2O_3$ systems were designed and prepared in this study. Glasses and glass-ceramics suitable for relatively high temperature applications were developed. The following conclusions can be deduced.

1. Many new compositions were found to be suitable for the casting of crack-free, optically clear glasses with glass transition temperatures ranging from 595 to 775 °C. Their colors ranged from brown to blue.
2. For glasses with the composition of $\alpha(SrO \cdot TiO_2)\beta B_2O_3 \cdot \gamma SiO_2(1-(\alpha+\beta+\gamma))Al_2O_3$, aluminoborate (G2) glasses exhibited the lowest process and glass transformation temperatures (T_g's), aluminosilicate (G8) glasses exhibited the highest T_g's, and borosilicate (G4–G6) glasses could not be cast.
3. The addition of P_2O_5 into G2, G10, and G12 glasses consistently decreased T_g and T_d values (T_g values also decreased in G8 glasses) indicating decreased viscosity and cross-linking in the structure.
4. The addition of P_2O_5 into G2, G8, and G12 glasses decreased the crystallization temperature, indicating easier crystallization due to P_2O_5 acting as a nucleating agent. However, P_2O_5 acted in the opposite way in G10 glasses demonstrated by higher crystallization temperatures upon increased P_2O_5 additions.
5. Glass-ceramics can be produced using a single-step heat treatment at temperatures of 750–800 °C with G2, G10, and G12 compositions. G8 compositions required higher temperatures (>1,000 °C) for transformation.

Acknowledgements Bengisu expresses his thanks to Dr. S. Reis from the Graduate Center for Materials Research at the University of Missouri-Rolla for his helpful comments, to Prof. C. Isci from Yasar University for his help with density measurements, and to Prof. S. Karadeniz from 9 Eylul University, Department of Mechanical Engineering, for his help with hardness measurements.

References

1. Donald IW (1993) J Mater Sci 28:2841
2. Tummala RR (1990) In: Nair KM (ed) Glasses for electronic applications. American Ceramic Society, Westerville, OH, p 419
3. Brow RK, Watkins RD (1992) US Patent 5,104,738, April 14
4. Tuller HL, Button DP, Uhlmann DR (1980) J Non-Cryst Solids 40:93
5. Donald IW, Metcalfe BL, Bradley DJ, Hill MJC, McGrath JL, Bye AD (1994) J Mater Sci 29:6379
6. Pereira TAS, Freire JAK, Freire VN, Farias GA, Scolfaro LMR, Leite JR, Da Silva EF Jr (2003) Microelectr J 34:507
7. Lawless WN (1972) Ferroelectrics 3:287
8. Swartz SL, Bhalla AS (1986) Mater Res Bull 21:1417
9. Thakur OP, Kumar D, Parkash O, Pandey L (1995) Bull Mater Sci 18:577
10. Thakur OP, Kumar D, Parkash O, Pandey L (2003) Mater Chem Phys 78:751
11. Mosel G, Willfahrt M, Banach U, Hübert Th (1997) J Mater Sci 32:1591
12. Brochu M, Gauntt BD, Shah R, Miyake G, Loehman RE (2006) J Eur Ceram Soc 26:3307
13. Swartz SL, Breval E, Randall CA, Fox BH (1988) J Mater Sci 23:3997
14. Swartz SL, Breval E, Bhalla AS (1988) Am Ceram Soc Bull 67:763
15. Sahu AK, Kumar D, Parkash O, Thakur OP, Prakash C (2004) Ceram Int 30:477
16. Klyuev VP, Hubert T, Banach U, Kirsch M, Bulaeva AV (1989) In: Mazurin OV (Ed) Properties of glass, new methods of glass formation, 15th International Congress on Glass. I.V. Grebenshchikov Institute of Silicate Chemistry, Academy of Sciences of the USSR, Leningrad, p 341
17. Bengisu M, Brow RK, Yilmaz E, Moguš-Milanković E, Reis ST (2006) J Non-Cryst Solids 352:3668
18. Fang X, Ray CS, Mogus-Milankovic A, Day DE (2001) J Non-Cryst Solids 283:162
19. Kataoka Y (1989) Rigaku J 6:33
20. Shelby JE (2005) Introduction to glass science and technology. Royal Society of Chemistry, Cambridge, UK
21. Ramkumar J, Sudarsan V, Chandramouleeswaran S, Shrikhande VK, Kothiyal GP, Ravindran PV, Kulshreshtha SK, Mukherjee T (2008) J Non-Cryst Solids 354:1591
22. Metwalli E (2003) J Non-Cryst Solids 317:221
23. Bengisu M (2001) Engineering ceramics. Springer Verlag, Heidelberg
24. Ray CS, Day DE (1997) J Am Ceram Soc 80:3100
25. Doremus RH (1994) Glass science. Wiley, New York